The SRTM Sub-arcsecond Metrology Camera

Riley M. Duren and Carl C. Liebe
Jet Propulsion Laboratory
California Institute of Technology
4800 Oak Grove Drive
Pasadena, CA 91109-8099
818-354-5753
Riley.M.Duren@jpl.nasa.gov

Abstract - To achieve the necessary interferometric baseline for the recent Shuttle Radar Topography Mission (SRTM), an outboard radar antenna was deployed using a 60 meter mast from a main radar antenna in the shuttle payload bay. The mast had dominant flexible modes around 0.1 Hz with tip displacements on the order of several centimeters in response to shuttle thrusters. Continuous knowledge of the mast tip position to sub-millimeter accuracy and antenna orientation to an accuracy of 100 arcseconds (1.6 sigma) was necessary to meet the fundamental SRTM requirements. The selected approach involved an optical metrology camera which tracked three LED targets located on the outboard antenna structure. The metrology camera was required to generate target centroid coordinates (in CCD frame) with a relative accuracy of 0.8 arcsec, 1 sigma. This paper provides a description of the metrology camera, the process used to prepare it for flight on SRTM, the LED target development effort, test and alignment issues, and the observed in-flight performance.

TABLE OF CONTENTS

1. INTRODUCTION & SRTM OVERVIEW

The Shuttle Radar Topography Mission (SRTM) payload was flown on the Shuttle Endeavor STS-99 February 11-22, 2000. Interferometric Synthetic Aperture Radar (IFSAR) techniques were used to successfully acquire data necessary for generating a topographic map covering 80% of the earth's land surface. The SRTM data will be used to create a digital model of the Earth that will satisfy the National Imaging and Mapping Agency (NIMA) Digital Terrain Elevation Data Level 2 (DTED-2) requirements, which specify 10 meter relative (over a scene) vertical height accuracy, 16 meter absolute vertical height accuracy, and 30 meter postings (1.6 sigma). These will provide unprecedented insight into the Earth's surface topography, with myriad uses spanning the scientific, commercial, and military sectors of remote sensing [1].

To achieve the necessary interferometric baseline, an outboard radar antenna was deployed using a 60 meter mast, the largest rigid structure ever flown in space, from a main radar antenna in the shuttle payload bay. While fairly rigid, the mast nonetheless behaved as a flexible structure with tip displacements on the order of several centimeters in response to shuttle thrusters. Knowledge of the mast tip position to sub-millimete and mast tip orientation to an accuracy of 100 arcseconds (1.6 sigma) was required in order to meet the baseline metrology error budget (a key to meeting the overall height accuracy) and to support on-orbit alignment of the two radar antennas. Knowledge of mast motion was also necessary in order to perform on-orbit system identification of the mast/shuttle system to optimize the shuttle's attitude control system and to verify mast integrity was sufficient to meet safety requirements during orbit trim maneuvers. The SRTM Attitude and Orbit Determination Avionics (AODA) subsystem was responsible for providing these measurements [2].

The solution consisted of an optical metrology camera which tracked three LED targets located on the outboard antenna structure. The state of the outboard antenna could be determined in 6 degrees of freedom using the metrology camera. However, due to physical constraints on LED target separation, the range component of mast tip position could not be determined to the required accuracy using the metrology camera alone. This required the addition of a rangefinder instrument, described elsewhere [3]. In order to meet the above system requirements, the metrology camera had to provide knowledge of target centroid position on the CCD with a relative accuracy of 0.8 arcsec, 1 sigma.

Providing sub-arcsecond accuracy given the tight SRTM schedule and budget constraints necessitated maximum reuse of existing hardware. The metrology camera was implemented as a modified version of the Advanced Stellar and Target Reference Optical Sensor (ASTROS), a sub-arcsecond star tracker developed by JPL in the 1980's and flown previously on the shuttle for the Astro-1 and –2 missions (STS-35 and –67). ASTROS was chosen due to its proven flight-worthiness and superior accuracy. The modifications included electronic and software changes to improve the tracking rate and additional optics to provide a 60 meter focus and stray-light rejection. The LED

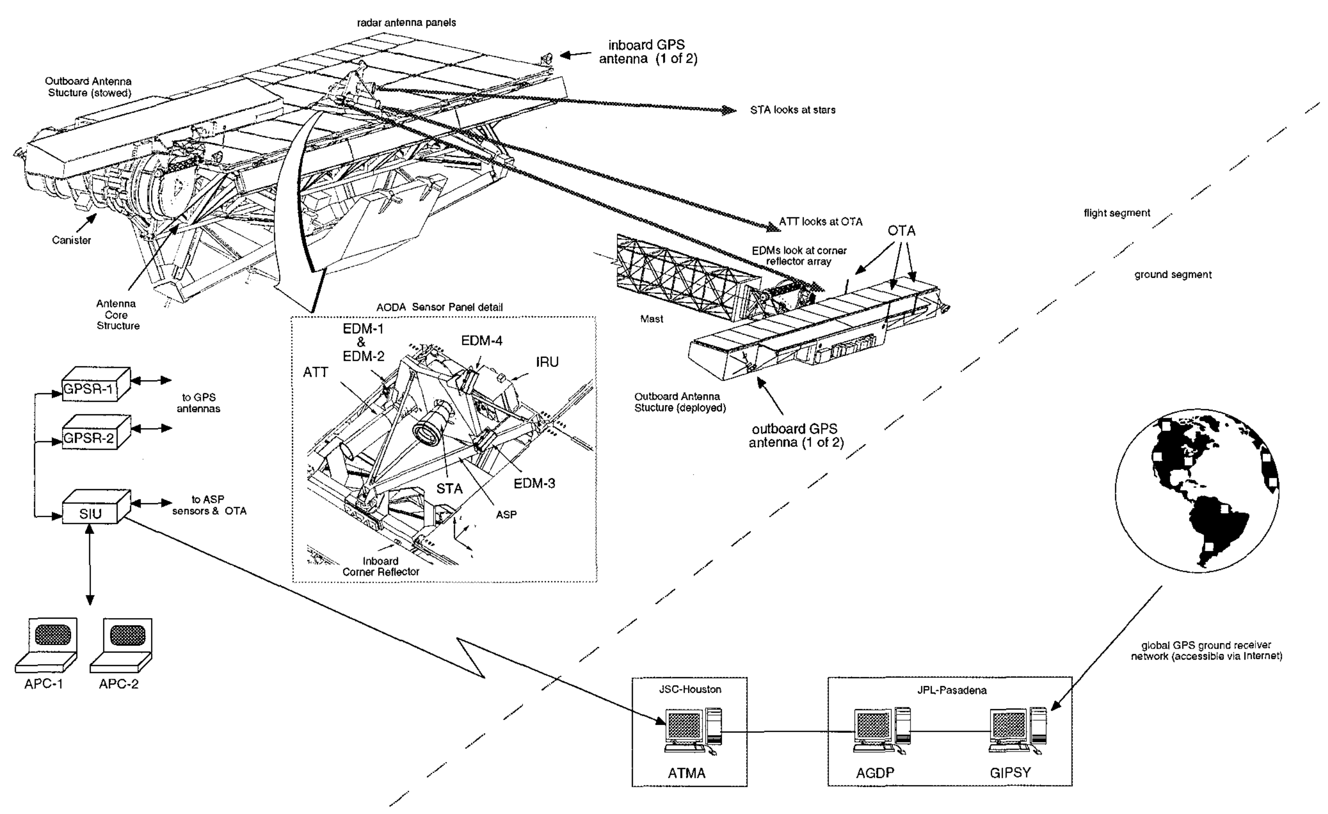

Figure 1 SRTM AODA Flight Configuration

targets consisted of commercial off-the-shelf LEDs mounted to the outboard radar antenna on custom-designed tubes. This paper provides a description of the metrology camera, the process used to modify it for flight on SRTM, the LED target development effort, test and alignment issues, and the observed in-flight performance.

2. SYSTEM REQUIREMENTS

The SRTM flight configuration is shown in Figure 1. It consisted of 4 primary subsystems: C-band radar, X-band radar, mechanical systems, and the Attitude and Orbit Determination Avionics (AODA). The mechanical system included a 60 meter deployable mast for providing the necessary interferometric baseline between the inboard and outboard radar antennas. Continuous knowledge of the combined shuttle/mast system's attitude and position was necessary to reconstruct the interferometric baseline and platform altitude which is critical to the topographic data processing effort. The AODA subsystem provided these attitude and position measurements. A brief description of the mast and AODA is provided as background.

The mast, developed by AEC-Able, was a composite structure composed of graphite epoxy longerons and battens with stainless steel fittings and titanium cables. When deployed, it formed a rigid structure with dominant natural frequencies on the order of 0.1 Hz. A portion of the deployed mast can be seen in Figure 2. The challenges of operating an interferometer on a dynamic platform like the shuttle with a large mast cannot be overstated. A few of these challenges are:

(1) The mast alone had very little inherent damping, resulting in the need to add viscous damper struts at the root to prevent resonant instability in response to the shuttle attitude control system. A complex process of inflight system identification was required to assess the stability and insure the safety of the shuttle and crew.

(2) Pointing of the radar antennas was affected by several factors involving the mast. Gravity unloading, launch shifts, and pre-flight assembly and alignment errors resulted in a quasi-static pointing bias. In-flight thermal distortions of the mast and antenna structures (bending and twisting) created pointing errors with time-constants of tens of minutes. Finally, the mast responded to the shuttle attitude control system thruster firings and astronaut crew activities. Mast bending resulted in relative misalignment between the two antennas (e.g., a 3 cm tip translation resulted in a 0.1° antenna misalignment).

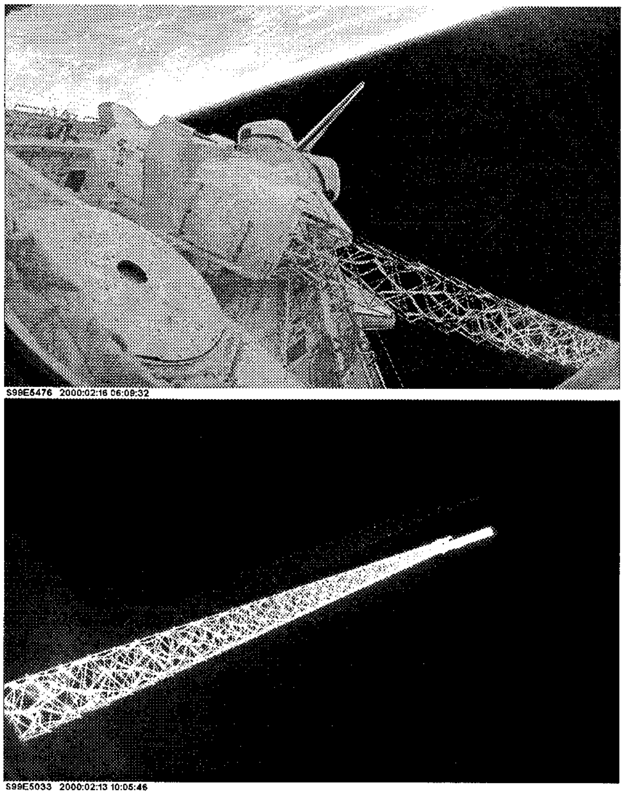

Figure 2 Inboard (top) and outboard (bottom) portions of the deployed mast

Although these challenges were mitigated by the SRTM structural and mechanisms design, mast pointing errors were ultimately dealt with by AODA and the radar instruments. Pointing errors affected the AODA and radar sensor's capability to both acquire and track targets.

The four basic AODA requirements were: 1) provide in-flight measurements necessary to verify successful mast deployment, 2) provide in-flight measurements necessary to guide alignment of the radar antennas, 3) provide updated measurements of mast modal frequencies to guide in-flight optimization of the Shuttle attitude control system, 4) provide data necessary to reconstruct the interferometric baseline vector during post-flight topographic data processing. These combined requirements resulted in 1 Hz, 1.6 sigma knowledge requirements for the outboard antenna relative attitude and position at the 100 arcsec and sub-mm levels, respectively.

A summary of the metrology camera and Optical Target Assembly (OTA) requirements is provided in Table 1. A brief description is provided here for each entry. In order to provide 5 degrees of freedom knowledge of the outboard antenna state, a minimum of 3 reference fiducials were needed on the outboard antenna structure. The 0.8 arcsec single-spot centroid accuracy was derived from the top-level requirement for antenna position and attitude knowledge. The 8 Hz frame rate was based on the predicted worst-case mast tip rates (6 cm/s) and an understanding of the metrology camera capability (having a one pixel per frame track limitation).

Requirement	**Specification (1 sigma)**
# of targets	3
tracker single-spot (centroid) accuracy	0.8 arcsec/axis
tracker frame rate (to track 6 cm/s mast tip dynamics)	8 Hz
tracker output data rate	4 packets/second
tracker data format	three 2-axis centroid coordinates and brightness measurements per packet
target position dynamic range (deployment errors)	59 ± 2 meters line of sight, ± 25 cm lateral
target brightness dynamic range	x6
target operating temp	-70 to +80 °C
tracker operating temp	0 to +40 °C
target boresight alignment	2 degrees/axis wrt tracker lens center
tracker alignment	0.01 deg/axis wrt target array centroid

Table 1 Metrology Camera and Target Requirements

The 4 frames/second was based on the available telemetry bandwidth and Nyquist sampling considerations. The data format is consistent with the need for 5 degrees of freedom knowledge of antenna state. The target position dynamic range represents the worst-case predicted mast tip deployment errors. The target brightness dynamic range represented the worst-case predicted variation in target intensity given the expected temperature swings, intrinsic brightness changes, and misalignments. The temperature requirements represent worst-case predicated excursions. The metrology camera was mounted on a temperature controlled cold plate whereas the targets were "hanging in the breeze" on the outboard antenna with no significant blanketing and therefore exposed to frequent orbital sunlight changes (orbit period = 90 minutes). The target boresights needed to be pointed at the metrology camera to maximize signal to background ratio (given their fairly narrow beam-width). The metrology camera needed to be pointed precisely to insure there was sufficient FOV margin for mast deployment errors and to minimize biases for inflight use of the data.

3. OPTICAL TARGET ASSEMBLY

Target Selection and SNR Considerations

One of the most important considerations in designing this metrology system was to insure a high SNR between the target sources and the background of the sky and outboard antenna structure. This is necessary for reliable target acquisition and best tracking performance. Three methods were used to meet this requirement.

- Bright Targets. It is desirable to have very bright optical sources. At the same time, the source must be small and have a point source appearance so the camera can properly centroid on it [4]. Lasers are very bright and their monochromatic nature is also attractive. However, they were not suitable for this application due to several issues: large predicted temperature variations of the outboard structure (-70°C to +80°C) presented stability challenges, the coherent nature of the laser light could potentially generate unpredicted effects in the tracker optics, and significant work would be required to insure eye safety for the shuttle crew. It was therefore decided to instead use a very bright red AlInGaP LED from HP: HLMP-DG08 [5]. It has a dominant wavelength of 626 nm, a spectral half-width of ±17 nm, and a luminous intensity of 2900-6500 mcd at 20 mA. The effective beam-width (half-angle) is 6°.

- Bandpass Filtering. The primary source for illumination of the outboard antenna is the sun, which is approximately a black body radiator of 5800°K. Unfortunately, a large portion of the solar flux is distributed across the same visible wavelengths to which the tracker is sensitive (390-770 nm). So it is important to take advantage of the fairly narrow bandwidth of the LED targets (609-643 nm) and attenuate solar illumination using a bandpass filter on the metrology camera. However, there is a limit to how narrow the filter can be. Light from an LED and the passband of an optical filter change with temperature. A test at JPL showed that a similar type LED exhibited a 10 nm spectral shift associated with a 60°C temperature change. If the passband on the filter is too narrow, the LED can shift out of it as the on-orbit ambient temperature changes. Ultimately, a narrow-band interference filter was selected with a center wavelength of 638 nm and a FWHM of 34 nm. This filter was challenging to find given the large camera aperture (4 inch) and our wavefront distortion tolerances (optics good to <= $\lambda/4$). We obtained a narrowband interference filter filter from Barr Associates who used a process similar to the one employed for the filters they provided for the Hubble Wide Field Planetary Camera.

- Dim Background: Even with the selection of bright sources and filtering, the remaining background due to solar illumination of the outboard antenna was still formidable. In particular, specular reflections due to glint on the metal antenna structures could easily exceed the intensity of the LED targets and thus present a confusion source. Initially, attempts were made to select black thermal blankets for the portion of the outboard antenna in the metrology camera Field of View (FOV) as opposed to the more thermally desirable white blankets. It is not only important that the material is black, it must also be optically flat in order to avoid specular reflection. Great effort was spend on finding the appropriate material to wrap around the outboard structure. A delicate balance had to be made between the thermal and optical characteristics of the blankets. The material with the best opto-thermal properties was black painted kapton. Unfortunately, this material did not prove robust enough for space flight (the paint flaked off over time and presented a contamination source). Ultimately, the decision was made to use black beta cloth instead. A photo showing a portion of the outboard antenna (covered in black beta cloth) and the illuminated OTA is provided in Figure 3.

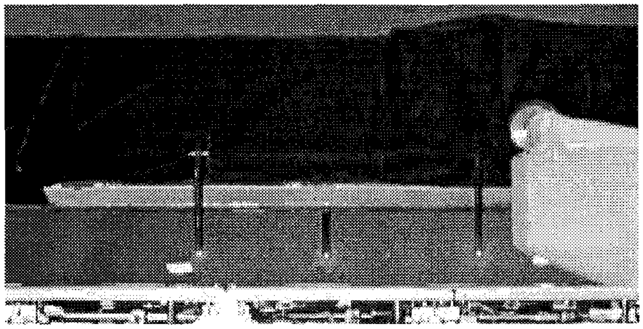

Figure 3 Optical Target Assembly (OTA)

OTA Thermal Considerations

The wavelengths and brightness of an LED changes with temperature. The relative brightness of the optical sources was therefore characterized over temperatures behind the bandpass filter. The experiments were conducted in a nitrogen oven. The light was transmitted out of the oven though an optical fiber bundle. The brightness as a function of temperature is shown in figure 4.

Due to the potential brightness variations, it was decided to have a feedback loop on the brightness. When the metrology camera reported that the brightness was too high, the current was reduced (and vice-versa).

Other OTA design issues

A total of three OTA arrays were flown, each consisting of 3 LEDs. The primary array was used during nominal SRTM data-taking operations (mast and outboard antenna deployed). The backup array was flown but never used during the mission. The outboard antenna was stowed in an "upside down" configuration during launch, landing, and mast deploy/stow operations. This required the use of a stow array (with LEDs pointing approximately 180 degrees away from the primary and backup array LEDs) so that the metrology camera could monitor mast and antenna deployment with the antenna in the stowed orientation. Only one OTA array was operated at a time.

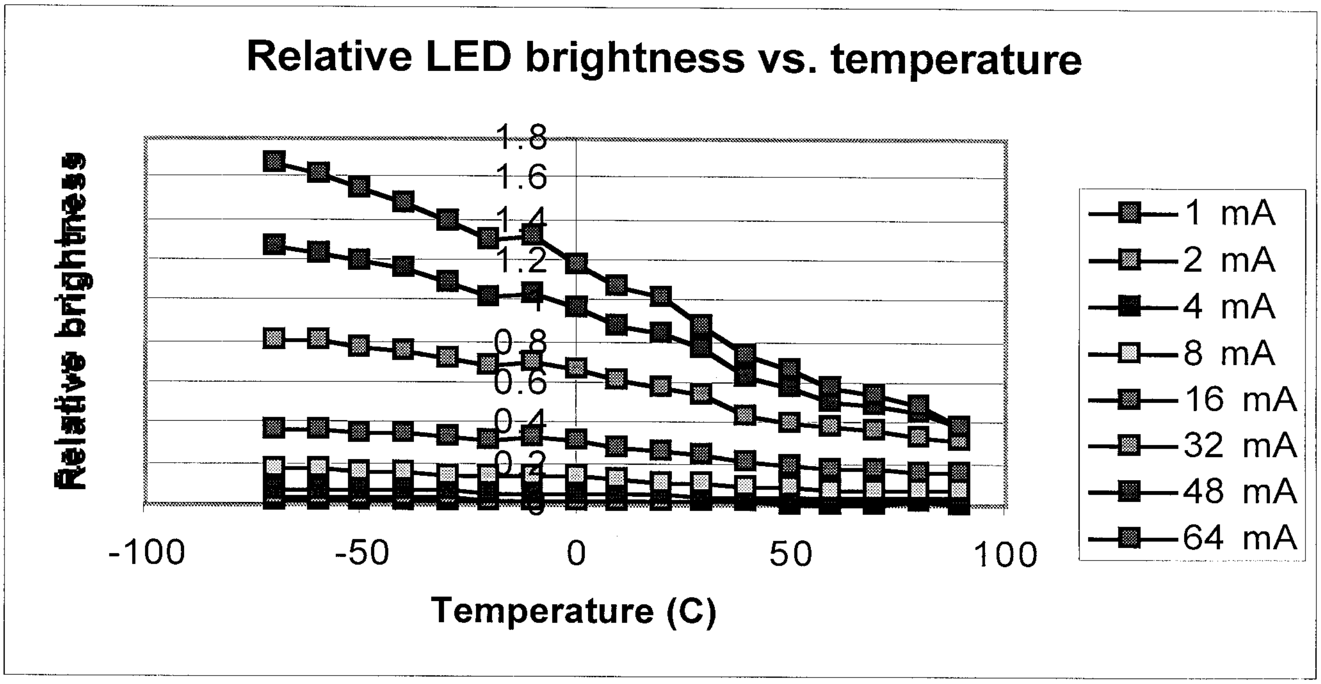

Figure 4 LED brightness vs temperature

As shown in Figure 5, three hollow stalks composed of a graphite-cyanate composite were mounted to the outboard antenna structure. Each OTA array consisted of an LED on each stalk. The LEDs in each array were wired in series (to insure consistent intrinsic brightness) and driven by a current source in the AODA electronics on the main antenna. The brightness could by varied by commanding changes in the current driver. This was done manually and also by brightness control software in one of the onboard AODA computers which servoed the LED drive current to maintain the target brightness sensed by the metrology camera in a predefined deadband.

4. ASTROS TARGET TRACKER (ATT)

Primarily based on budget and schedule constraints it was decided to modify the existing Advanced Stellar and Target Reference Optical Sensor (ASTROS) star tracker to track the OTA. For SRTM this was referred to as the ASTROS Target Tracker (or ATT, as seen in Figure 1). The ASTROS star tracker was originally a part of the Astro-1 and Astro-2 shuttle missions. It was a pioneering CCD based star tracker, designed in the beginning of the 1980's. Photos of the ASTROS star tracker are shown in figure 6 (sensor on the top, processing electronics on the bottom) [6], [7].

It was necessary to modify the optics to track bright red optical sources at 60 meters instead of dim stars at infinity and also increase the acquisition and the track speed (ASTROS was originally designed to operate on a gimbaled pointing platform which relaxed the need to track fast-moving targets). Applying a corrective lens and a passband filter in front of the star tracker lens modified the optics. The corrective lens for focusing at 60 m instead of infinity was a plano-convex lens. The lens had a 4-inch clear aperture and was 0.5 inches thick. It was

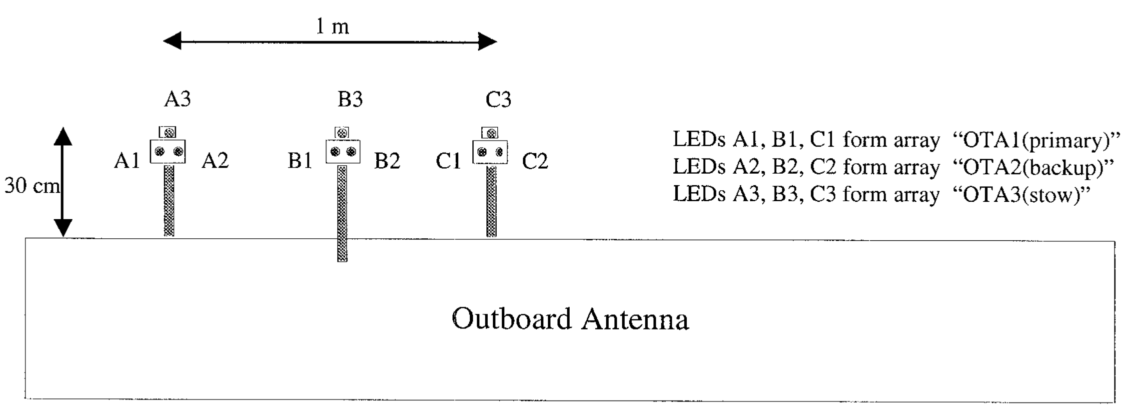

Figure 5 OTA Arrays

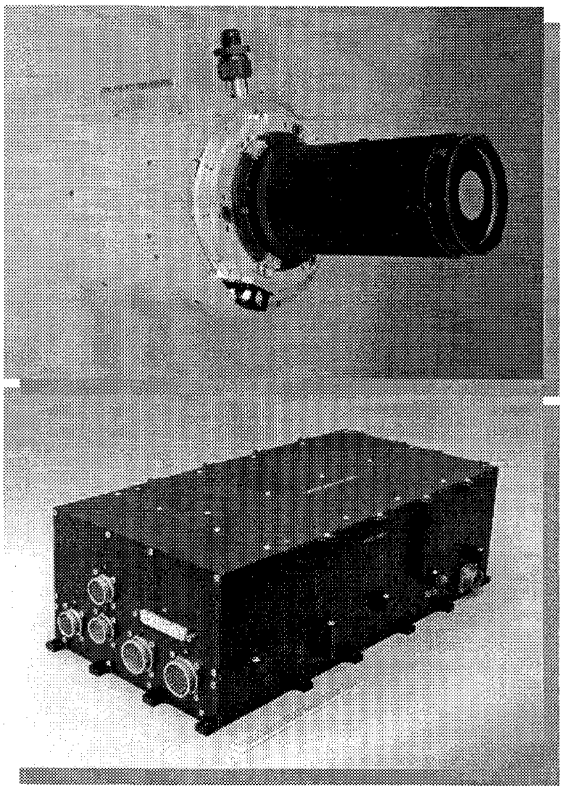

Figure 6 ASTROS sensor (top) and electronics (bottom)

fabricated at JPL and made of fused quartz. It is difficult to grind a lens to focus at 60 meters given the large radius of curvature (30 meters). Therefore, an iterative process of testing was required to assess the image quality and make small adjustments to find the optimum lens figure. Finally the corrector lens received anti-reflective and neutral density coatings to attenuate the light from the bright LEDs to 1/725. This was selected to provide the maximum dynamic range for the system (i.e., the LEDs at room temperature are too bright for the tracker but margin was provided for thermally driven brightness changes). As mentioned previous, a bandpass filter was also installed in front of the optics.

ASTROS has limited processing capabilities compared to modern star trackers. Therefore, both hardware and firmware modifications had to be done. The clock speed of the fast horizontal clock (clocking when there are no window data) was increased so the frame time were decreased from 92 ms to 52 ms. Also, modifications in the firmware had to be done. Primarily in the initial target acquisition. The originally firmware expected stars with very different brightness. In this application, the brightness was known apriori, so small modifications to these algorithms had to be performed. After the modifications, the camera was capable of tracking as fast as 12 Hz but was typically operated at 8 Hz for best performance. The exposure time was set for 15 ms. Given the short exposure time, dark current was insignificant and therefore thermo-electric cooling of the CCD chip was not required.

5. CALIBRATION & ALIGNMENT

Absolute Calibration

The optimal position for the target image is close to the center of the field of view, because that region affords the best accuracy and it is more likely that the targets will stay in the field of view. Therefore it was necessary to perform an absolute calibration of the metrology camera. Absolute calibration involves generating a mathematical model of the metrology camera so it is possible to predict where points in a Cartesian xyz coordinate system (related to the alignment cube on the metrology camera) will be imaged on the focal plane array. For this purpose a calibration light bar was manufactured. The calibration light bar consisted of 15 LEDs. A sketch of the calibration light bar is shown in figure 7.

The metrology camera recorded the positions of the LEDs in focal plane coordinates. The positions were also measured simultaneous with a total station (in a xyz coordinate system related to the alignment cube). Two measurements of the calibration light bar were made at different distances, for a total of 30 measurements. A simple pinhole camera was assumed for the mathematical model. A sketch of the model is shown in figure 8.

In the simplified model, it is assumed that the focal plane is oriented with the coordinate system of the alignment cube and that no additional rotations are required. The equations for transforming a Cartesian coordinate into a focal plane array coordinate are shown below.

There are 6 unknowns, $x_{\text{translation from alignment cube to pinhole}}$, $y_{\text{translation from alignment cube to pinhole}}$, $z_{\text{translation from alignment cube to pinhole}}$, F (focal length) $x_{\text{translation from pinhole to CCD}}$ and $y_{\text{translation from pinhole to CCD}}$,

$$\begin{pmatrix} x_{LED,pinhole\,CS} \\ y_{LED,pinhole\,CS} \\ z_{LED,pinhole\,CS} \end{pmatrix} = \begin{pmatrix} x_{LED,alignment\,cube\,CS} \\ y_{LED,alignment\,cube\,CS} \\ z_{LED,alignment\,cube\,CS} \end{pmatrix} + \begin{pmatrix} x_{translation\,from\,alignment\,cube\,to\,pinhole} \\ y_{translation\,from\,alignment\,cube\,to\,pinhole} \\ z_{translation\,from\,alignment\,cube\,to\,pinhole} \end{pmatrix}$$

$$\begin{pmatrix} x_{LED,focalplane,pinhole} \\ y_{LED,focalplane,pinhole} \end{pmatrix} = \begin{pmatrix} -x_{LED,pinhole\,CS} / z_{LED,pinhole\,CS} \cdot F \\ -y_{LED,pinhole\,CS} / z_{LED,pinhole\,CS} \cdot F \end{pmatrix}$$

$$\begin{pmatrix} x_{LED,ccd} \\ y_{LED,ccd} \end{pmatrix} = \begin{pmatrix} x_{LED,focalplane,pinhole} \\ y_{LED,focalplane,pinhole} \end{pmatrix} + \begin{pmatrix} x_{translation\,from\,pinhole\,to\,ccd} \\ y_{translation\,from\,pinhole\,to\,ccd} \end{pmatrix}$$

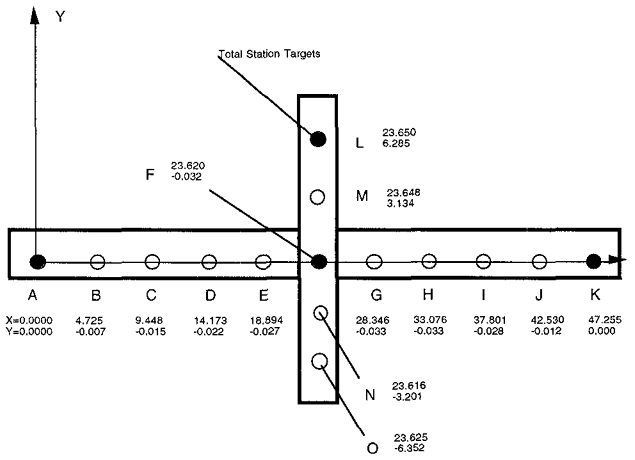

Figure 7 Absolute calibration light bar

There are 30 LED measurements = 30 equations. This set of equations can easily be solved with Matlab or with the Excel solver. The solution had an average accuracy of 0.077 pixels. This is the absolute accuracy. This should not be confused with the relative accuracy, which is much better.

Optical Target Alignment

Most metrology cameras provide optimal performance over a given target brightness range. It is therefore important that the different optical sources have equivalent brightness. Considerable effort was required to align the LED targets so that they were all pointing accurately toward the metrology camera.

S-curve correction

Star trackers and other instruments that image point sources are effected by a phenomenon known as s-curve. The s-curve is an artifact of the sampling theorem. As an example, suppose that a star is focused perfectly with an infinitely small point spread function. Since it is not possible to determine where on a pixel that the photons are hitting, the average accuracy of this instrument would be (in pixels):

$$\int_{-0.5}^{0.5}\int_{-0.5}^{0.5}\sqrt{x^2+y^2}\,dxdy = 0.38$$

On the other extreme, if the star/target is smeared out over a large number of pixels, it is possible to calculate the centroid of light with no systematic error. In most instruments the situation lies somewhere between the two extremes and a pixel-peroidic correction will have to be applied to the decimal part of the centroid. This is called an s-curve correction. Analysis of data acquired during the SRTM mission indicates and s-curve correction needs to be made for the metrology camera. This correction can be derived by calibration of the effect using the metrology camera itself (i.e., by dithering a target image across pixels with idependent position knowledge and solving for the s-curve). This effort is currently underway.

6. FLIGHT PERFORMANCE

Mission Highlights

The metrology camera was activated three hours after launch and was operated continuously for almost 10 days. Initially, proper functionality was successfully verified using the internal test star. During the later stage of mast deployment the metrology camera was put in Acquisition Mode to acquire the OTA stow array targets as they came into the field of view. At first there were several spurious acquisitions of targets which did not match the expected positions. These were most likely the result of sun glint on the outboard antenna structure (expected behavior given some bright structures on the flip side). By the end of mast deployment, all three targets were acquired and the observed coordinates correlated well with the predicted OTA target positions and separations. The OTA primary array was then switched on, which was successfully acquired following the flip-deploy of the outboard antenna. The metrology camera remained locked on the OTA targets for the remainder of the flight, with the exception of the high impulse thruster test and the orbit trim burns (generally once per day). During those times the metrology camera lost track during the period of rapid OTA motion as the mast reacted to the shuttle thrusters, as expected from pre-flight predictions. Recovery was always prompt (< 30 seconds to reacquire targets).

The ambient temperature of the metrology camera corrector plate (optics temp) was lower than predicted, resulting in the default optics heater setpoint being too high (i.e., heater was running constantly). Therefore, several tweaks of the optics heater setpoint were made to reduce the delta between the surrounding temperature and the setpoint. Optics temperature stability was extremely good (about 0.1 degC RMS).

Alignment & Tracking

A key to optimizing metrology camera performance was achieving a good alignment of the system. Maximum accuracy is achieved when the targets lie near the center of the CCD. Figure 9 shows the actual location of the OTA targets on the metrology camera CCD which indicates that the inflight alignment was nearly perfect. It also indicates typical target motion (in pixels). For scale reference, the metrology camera FOV subtends about 2.5 x 3.2 meters at 60 meters.

Figure 10 depicts typical dynamics for a 5 minute interval of shuttle thruster firings on a single target representing about 10 cm of motion peak to peak in the Z (vertical) axis. Units are in pixels (one pixel = 7.3 mm at 60 meters).

The in-flight performance/accuracy of the metrology camera was estimated as follows:

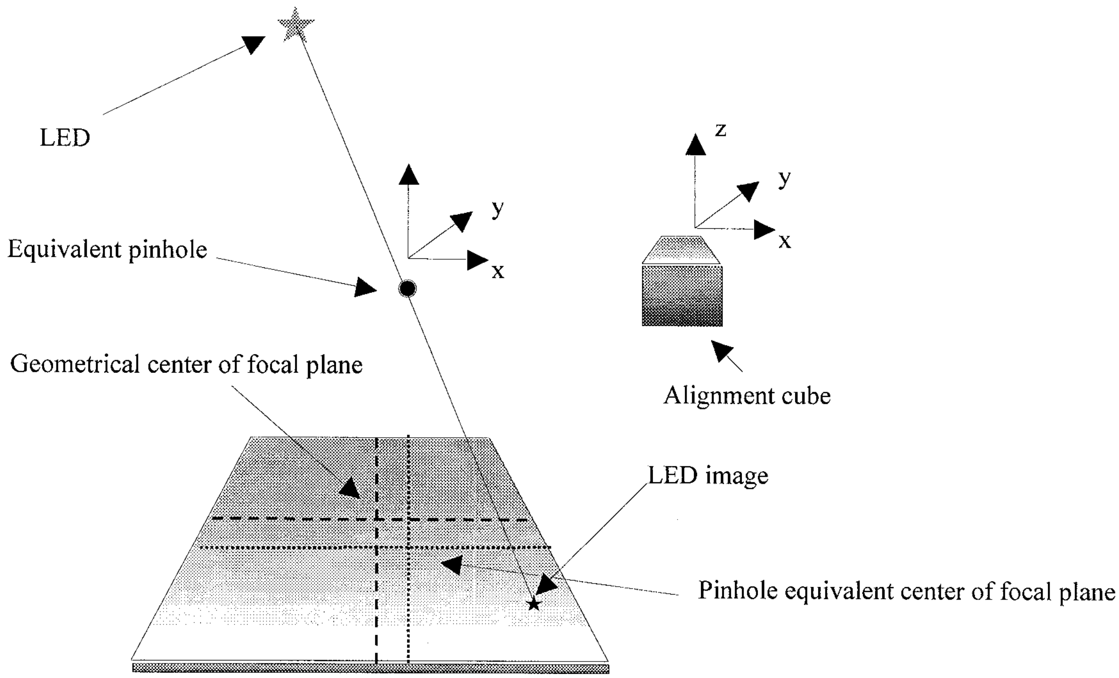

Figure 8 Simple model for absolute calibration

a. A 5 minute snap-shot of Line & Column data for all three targets was acquired. Since the metrology camera data is sampled at 4 Hz, this results in 1200 samples of each quantity.

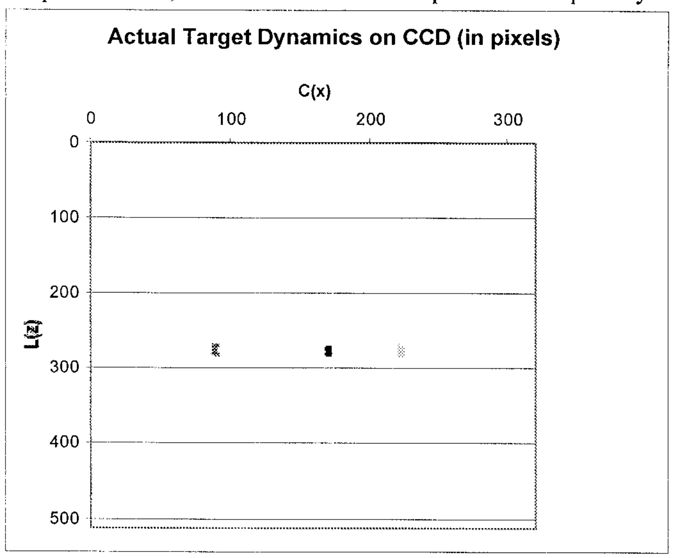

Figure 9 Target positions on FOV

b. The vector between the outer two OTA targets was then calculated. The middle target must be ignored as rotations of between the two outer targets is more or less rigid so any noise observed is primarily metrology camera-induced (which is what we want to observe).

c. Finally, the standard deviation in the vector over the sample space was calculated.

Figure 11 depicts a 5 minute plot of metrology camera sensor noise (i.e., the separation vector between the two outer targets). The noise has a standard deviation of 0.0094 pixel. The distance from one optical source to another optical source includes errors from both sources. Therefore the standard deviation can be divided with sqrt (2) to find the error on a singe optical source. One pixel is equal to ≈24.8 arcseconds. The RMS accuracy of a single target is therefore ≈0.18 arcseconds or a stunning ≈50 microns at 60 meters. This is much better than the required 0.8 arcsec accuracy requirement.

7. SUMMARY

This paper described the metrology camera and optical target assembly used on the SRTM mission. The conversion of an existing high precision star tracker into a sub-millimeter accuracy metrology system was discussed. The system provided single-spot target position knowledge at the 0.2 arcsec (1 sigma) level for a 60 meter deployed flexible structure on the space shuttle. S-curve correction must be completed before the final accuracy is known. However, all indications are the metrology camera accuracy will be better than the requirements thus providing improved overall height accuracy for the SRTM global topographic data set.

ACKNOWLEDGEMENTS

The authors thank Phil Salomon, Ed Dennison, Bob McMillan, Morris Birnbaum, Jeffrey Schroeder, Jim Alexander, and Edward Litty for valuable contributions to this effort.

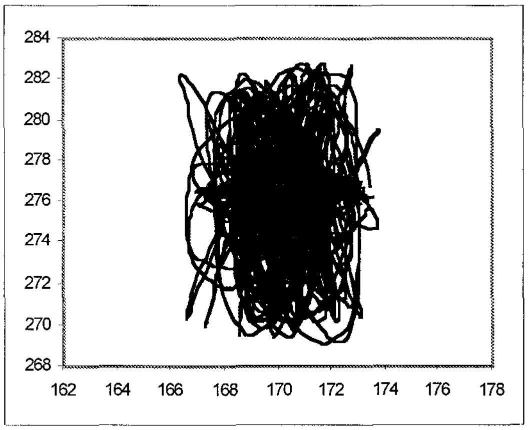

Figure 10 Target dynamics (in pixels)

The research described here was carried out at the Jet Propulsion Laboratory, California Institute of Technology, and was sponsored by the National Aeronautics and Space Administration. References herein to any specific commercial product, process or service by trademark, manufacturer, or otherwise, does not constitute or imply its endorsement by the United States Government or the Jet Propulsion Laboratory, California Institute of Technology.

9. References

[1] Jordan, Rolando L; Caro, Edward R; Kim, Yunjin; Kobrick, Michael; Shen, Yuhsyen; Stuhr, Frederick V; Werner, Marian U: Shuttle radar topography mapper (SRTM), Microwave sensing and synthetic aperture radar; Proceedings of the Meeting, Taormina, Italy, Sept. 23-26, 1996, (A97-18926 03-35), Bellingham, WA, Society of Photo-Optical Instrumentation Engineers (SPIE Proceedings. Vol. 2958), 1996, p. 412-422.

[2] Duren, Riley; Wong, Ed; Breckenridge, Bill; Shaffer, Scott; Duncan, Courtney; Tubbs, Eldred; Salomon, Phil: Metrology, attitude, and orbit determination for spaceborne interferometric synthetic aperture radar, Acquisition, tracking, and pointing XII; Proceedings of the Meeting, Orlando, FL, Apr. 15, 16, 1998 (A99-13701 02-63), Bellingham, WA, Society of Photo-Optical Instrumentation Engineers (SPIE Proceedings. Vol. 3365), 1999.

[3] R. Duren, E. Tubbs, "A Modified Commercial Surveying Instrument for Use as a Spaceborne Rangefinder", *Proceedings of the IEEE*, Aerospace Conference,18-25 March 2000.

[4] Phil Salomon, "Charge-Coupled Device (CCD) trackers for high-accuracy guidance applications", 1987, SPIE Vol 203, p. 130.

[5] http://www.avnet-pacific.com/hew/AlInGaP.htm

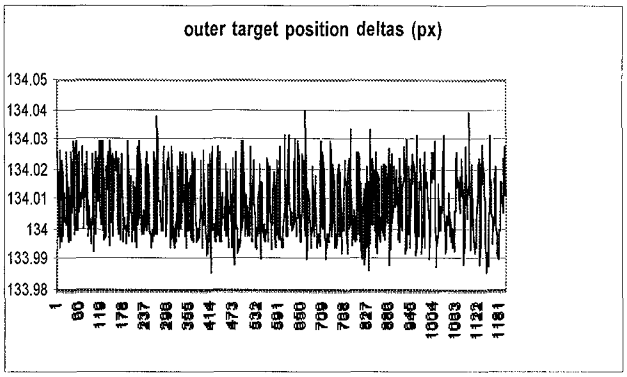

Figure 11 Metrology camera measurement noise

[6] R.H.Stanton et al: ASTROS: A sub-arcsec CCD Star Tracker, SPIE/Vol. 501, State of the Art Imaging Arrays and Their Application (1984).

[7] E.Shalom, J.W.Alexander and R.H.Stanton: Acquisition and track Algorithms for the ASTROS star tracker, American Astronautical Society, Annual Rocky Mountain Guidance and Control Conference, February 2-6, 1985, Keystone Colorado, AAS 85-050.

10. Biography

Riley Duren received a BSEE in 1991 from Auburn University. He also studied astronomy and physics at UCLA and the Florida Institute of Technology. He worked for NASA at the Kennedy Space Center from 1988-1995, where he prepared five space shuttle science instruments for flight. He joined JPL in 1996 where he served for 4 years as the lead system engineer for the SRTM Attitude and Orbit Determination Avionics as well as and was one of the SRTM Mission Operations Directors. He is currently the Instrument System Engineer for the Space Technology 3 (ST3) mission, a formation-flying stellar interferometer precursor for the Terrestrial Planet Finder project. His interests include the search for extra-solar terrestrial planets and space-based interferometric instrumentation.

Carl Christian Liebe received a MSEE in 1991 and a Ph.D. in 1994, both from the Department of Electro-physics, Technical University of Denmark. Since 1997, he has been a member of the technical staff at the Jet Propulsion Laboratory, California Institute of Technology. He has authored/co-authored more than 30 papers. He has performed research on a wide range of technologies associated with precision spaceborne electro-optical sensors. He played a key role in the development, test, and alignment of the metrology camera for the SRTM project. His current research interests are new technologies and applications for autonomous attitude determination and laser metrology.